Near-field optical observation of electric-field-induced fluorescence switching in laterally coupled quantum dots

Young-Jun Yu,* Haneol Noh,† and Wonho Jhe‡
Center for Nano-liquid and Department of Physics & Astronomy, Seoul National University, Seoul 151-742, Korea

Heung-Ryoul Noh
Department of Physics, Chonnam National University, Gwangju 500-757, Korea

Toshihiro Nakaoka and Yasuhiko Arakawa
Research Center for Advanced Science and Technology, University of Tokyo, Tokyo 153-8505, Japan
(Received 11 April 2010; revised manuscript received 24 June 2010; published 6 August 2010)

We report on direct observation of spatial and optical luminescence switching (*on* and *off* condition) due to collapse of the coupling conditions of quantum dots (QDs) pair. In particular, one could observe that the relative intensities between two adjacent luminescence peaks and spatial images of individual QDs located closely nearby in a high-density self-assembled QD structure underwent a reversible change with respect to an external electric field.

DOI: 10.1103/PhysRevB.82.085308 PACS number(s): 73.21.La, 68.37.Uv, 78.55.Cr, 78.67.Hc

I. INTRODUCTION

For experimental realization of robust quantum information systems, two-state quantum bit has been demonstrated by nonclassical light source materials[1–3] and controllable two states might be also materialize by semiconductor single quantum dots (QDs).[4–14] Especially, in order to study practical quantum gates, "quantum-dot molecules" have been articulately fabricated as "vertically"[5–7] or "laterally"[8,9] coupled semiconductor QDs. Self-assembled quantum dots, grown by molecular-beam epitaxy, are usually highly dense with a density larger than 10^{10} cm^{-2}. Such a high-density sample of QDs has been widely studied as a natural candidate for applications to nano-optical devices. Although the spectroscopic and microscopic characteristics of self-assembled single QDs have been studied extensively, coupling between single QDs in such a *high-density* sample has not been investigated, obviously since it is difficult to discriminate the spectral as well as the spatial properties of their split energy states. Therefore, it will be an interesting challenge and significant progress to study coupling between two adjacent self-assembled QDs because of its inherent practical potentials for nano and quantum applications. In this work, we report on the simultaneous, high-resolution photoluminescence (PL) spectroscopy and microscopy of laterally paired single QDs with electric field. In particular, by use of near-field scanning optical microscopy (NSOM), we have directly observed the electric-field-induced reversible variation in spatial luminescence distributions resulting from collapsing coupling between two nearby QDs.

II. EXPERIMENTS

The self-assembled InGaAs QDs was grown on the undoped GaAs buffer layer (100 nm)/*n*-doped GaAs substrate and then the QDs were capped by a 30 nm undoped GaAs layer. Here this QDs have an average lateral width of 23 nm, an average height of 6 nm, and a density higher than 8.2 $\times 10^9$ cm^{-2}. The atomic force micrographic (AFM) image in Fig. 1(a) provides the lateral sizes of QDs in Fig. 1(b). Note that, because of the lattice mismatch dependent on In-composition value of $In_xGa_{1-x}As$ QDs with the covering GaAs cap layer, one finds that the compressive stress to $In_{0.6}Ga_{0.4}As$ due to lattice mismatch with GaAs cap layer is around 5%, which is estimated from the reported value (Ref. 15) of 2.4% compressive stress of $In_{0.33}Ga_{0.67}As$ QDs in GaAs cap layer. The lateral sizes (red dots) shown in Fig. 1(b) were obtained by subtracting the measured size of AFM images without cap layer in Fig. 1(a) by the 5% correction

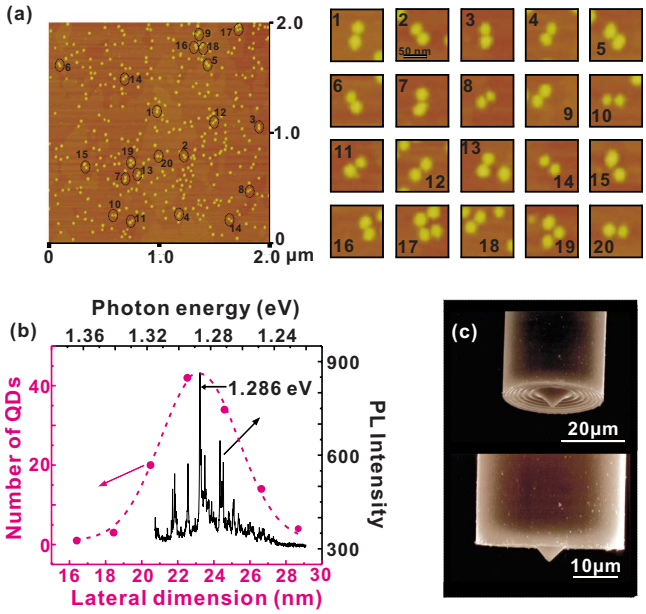

FIG. 1. (Color online) (a) AFM image of InGaAs QDs without GaAs capping layer (left) and the enlarged area of closely located QDs (right). (b) The lateral size distribution (red dots) and Gaussian fitting (broken red line) of QDs obtained from (a) while compared with the high-resolution PL spectrum (solid line). (c) Scanning electron micrographic image of the etched axicon lens probe.

 ©2010 The American Physical Society

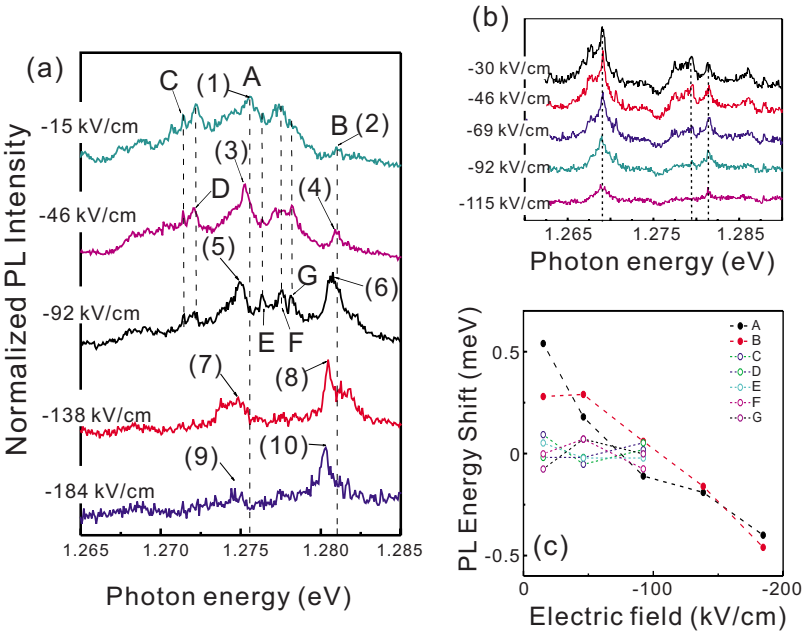

FIG. 2. (Color online) (a) PL spectra that show the reverse intensity change and energy shift of the PL peaks A and B with increasing the electric field unlike PL peaks C–G. (b) PL spectra that show the continuously intensity decreasing and unchange of energy with increasing the electric field. (c) Photon energy shift of PL peaks A–G under applying electric field of (a).

(corresponding to 1 nm) due to cap layer. And since the AFM tip size is much larger than a few nanometers, we could not directly obtain the exact lateral size and edge to edge distance between QDs. Nonetheless we could estimate the 23 nm average lateral size of QDs by Gaussian fitting [broken red line in Fig. 1(b)] of the QD sizes [red dots in Fig. 1(b)] measured from AFM images. And the 2–3 nm separation of QDs was estimated from the average values of the difference between the longitudinal size of coupled QDs [obtained from AFM images in Fig. 1(a)] and the twice of average single QD diameter (~46 nm). By comparing with the PL spectra associated with each QD, one can observe that the dominant PL peak is at 1.286 eV, as marked in Fig. 1(b), having the averaged lateral size of 23 nm of QDs. In Fig. 1(a), one can also find several regions where QDs are located closely nearby (2–3 nm average edge-to-edge distance).[9] A thin conducting Ti/Au coating of 20 nm thickness was made on the sample for biasing external electric field as well as optical excitation/detection. The electric field was varied from −15 kV/cm (~−0.2 V for the undoped thickness of 130 nm) to −184 kV/cm (~−2.4 V).

For optical excitation, we used the Ti:sapphire laser operating with 1.65 eV, which was coupled to a commercially available single-mode optical 2×2 fiber coupler and guided to a chemically etched optical "axicon" lens fiber tip, as shown by a scanning electron micrograph in Fig. 1(c). Note that, this optical axicon-lens fiber probe could focus light source and collect optical signal with a subwavelength spatial resolution (<400 nm).[16] Thus a nanoscale light source produced by the axicon lens probe could excite only a few tens of QDs by the shear-force distance control within several nanometers from the sample surface. The resulting PL signal was collected by the same axicon lens, which was dispersed by a 30-cm-long single monochromator with a spectral resolution of 70 μeV and detected by a liquid-nitrogen-cooled charge-coupled device. Both the sample and the axicon probe were enclosed in a gas-flow-type cryostat and kept at 77 K temperature, where it has been demonstrated that one can easily obtain the high-resolution NSOM spectral and spatial images.[17]

III. RESULTS AND DISCUSSION

The supplied electric-field direction was biased from top to bottom of our sample with grounded top gate and applied negative voltage to substrate. Usually, PL peaks are blueshifted or redshifted with releasing or more compressing the initially tilted potential well (PW) of QDs due to vertical sample structure dependent on electric-field direction. In our case, PL peaks should have been blueshifted with releasing PW under our electric-field direction. We, however, have not acquired the shifted PL peaks with electric field and we observed the PL intensity decrease with increasing electric field as shown at Fig. 2(b). From these results, we can consider the electric field as −30 to ~−100 kV/cm in our sample condition does not contribute to change vertical PW of QDs, but to turn down confinement of electrons at QDs. On the other hand, from the corresponding PL intensity variations between A and B in Fig. 2(a), it was observed that the PL intensity reversal between A and B occur at −92 kV/cm. And in Figs. 2(a) and 2(c), we checked the PL peaks A and B are redshifted by ~1 meV with the increase in electric field unlike the other PL peaks from C to G. From this evidence, we can make sure there is electric interaction between QDs A and B.

In Figs. 3(a)–3(f), we could clearly acquire the reversal intensity change feature between fitted PL peaks A and B without much of background signal. Since there are background signal and many mixed PL peaks, we could not clearly distinguish the characterized peaks as single exciton (X), biexciton (XX), or charged excitons (X^-,X^+). Thus, we have confined our study only on the clear results concerning PL peaks A (blue line) and B (red line) among fitted PL peaks in Fig. 3. It is also presented clear variations in the

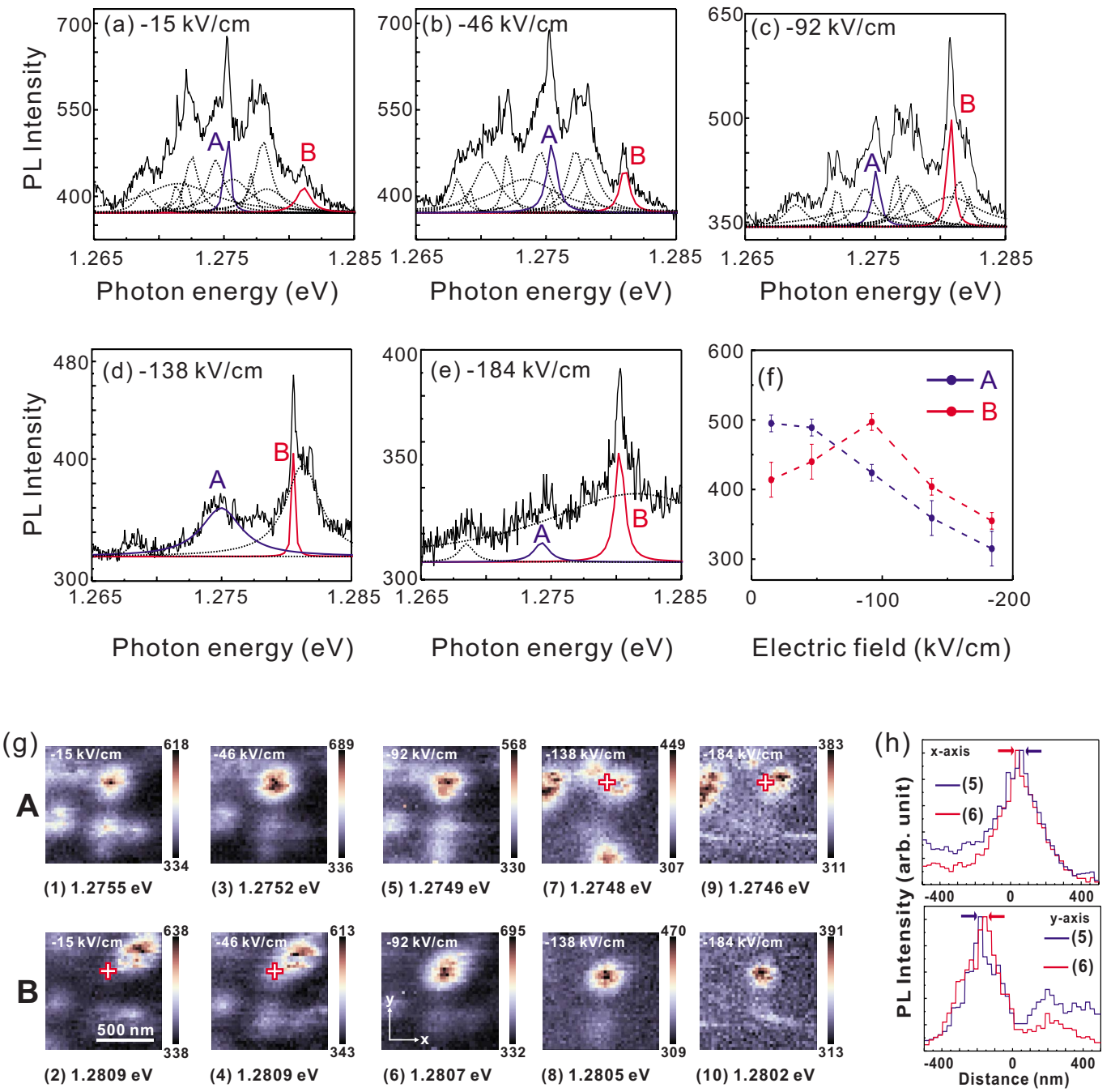

FIG. 3. (Color online) [(a)–(e)] Fitted PL peaks of Fig. 2(a) for obtaining intensity change in the PL peaks A (blue line) and B (red line) under the electric field variation without intensity supporting of background signal. (f) The intensity variation in A (blue dot) and B (red dot) of (a)–(e) as a function of applied electric field. (g) The corresponding spatial PL-intensity images for the respective PL energies of (1)–(10) in Fig. 2(a). The crosses in (2), (4) and (7), (9) represent the center of the PL intensity images of (6), (8), (10) and (1), (3), (5), respectively. (h) The corresponding spatial profiles of (5) and (6) in the x and y directions of (g) are presented, respectively.

spatial PL-intensity distribution of the QDs A and B for various electric fields in Fig. 3(g). The scanning images are obtained after reconstructing the collected optical signals at a given PL energy (scan area of 1 μm$\times$1 μm with a pixel size of 25 nm), as routinely done in our previous works.[17,18] We observe that as the electric field is increased from −15 to −46 kV/cm, only the PL-intensity image of A can be observed in Fig. 3(g), (1)–(4). However, at −92 kV/cm, the image of B appears in Fig. 3(g), (6) and it is brighter than A shown in Fig. 3(g), (5). The image of the QD A then disappears whereas that of B is still observed above −138 kV/cm as Fig. 3(g), (7)–(10).

The full width at half maximum of the $x(y)$-directional cross sections of the PL-intensity images of Fig. 3(g) is 186 nm (193 nm) in (1), 241 nm (234 nm) in (3), 235 nm (233 nm) in (5), 245 nm (241 nm) in (6), 222 nm (183 nm) in (8), and 161 nm (135 nm) in (10), respectively. Although the estimated spatial resolution of our system is about 135 nm

for 30-nm-thick capping layer, 20 nm Ti/Au electrode thickness and aixcon lens probe, one can distinguish the distance as small as 25 nm between the center positions of each QDs, as marked by the two arrows both in Fig. 3(h). Note that the differing scan images of Fig. 3(g), (5) and (6), as well as the differing spatial profiles in Fig. 3(h) indicate that the PL results from two independent neighboring QDs, representing the specific exciton wave functions of individual self-assembled semiconductor QDs.[18–20] Thus, one can observe that the PL peaks of A and B are not associated with the interlevel (i.e., X^-, X^+, and XX peaks[19–24]) of single QD but with two separate single QDs which are located closely nearby with each other [refer to the AFM image of Fig. 1(a)]. This accounts for the spatial variation in the radiative exciton distribution between coupled neighboring QDs A and B via the switching condition of the electric field at around −92 kV/cm.

For proper interpretation of the experimental results, we have calculated the potential and the electric field produced between two QDs having 23 and 24 nm lateral sizes and 2 nm (selected between 2–3 nm) average edge-to-edge separation in a vertically applied electric-field configuration[25,26] by assuming each QD is hemisphere shaped. In the calculation of the electric potential and field, we have used the fact that difference of the diameters of two QDs is much smaller than the diameter itself. Note that, these QD sizes could be assumed with setting the peaks A (1.275 eV) and B (1.281 eV) against Fig. 1(b). Figures 4(a)–4(c) show the contour plot of the potential, the vector plot of the electric field, and the cross-sectional profile of the electric field along the x axis, respectively, at the vertical electric field E_z of −92 kV/cm. Note that, in Fig. 4(b), the magnitude of the vertical components of the electric field are reduced by a factor of 10 in order to facilitate the visualization of the lateral electric-field components. In Fig. 4, one can observe that the lateral components are produced in the QD plane and these electric fields contribute to the electric-field-induced releasing tilted potential barrier of laterally coupled QDs, as schematically illustrated in Fig. 4(d). For our coupled QD structure, such as two QDs of 23 and 24 nm size at 2 nm average separation, it is suitable to employ the QD coupling conditions as used by previous results.[6–11] Beirne *et al.*[9] and Kawazoe *et al.*[10] also observed the coupling and the exciton tunneling phenomenon due to the Coulomb interaction of laterally neighbored QDs under no external electric field.[12] Although we could not observe experimental results at zero-electric field, it is clear that these QDs are already electrically coupled under −15 kV/cm electric field from Figs. 2 and 3. And moreover, in Figs. 3(a)–3(e), we could not observe the PL peaks which have intensity images matched with the PL peaks A and B. We, thus, could not observe doublet PL peaks represented bonding and antibonding states unlike our previous result.[18] This means there is nonradiative recombination in antibonding state and also indicates that, in Fig. 4(d), the dominant exciton is the radiative intradot exciton $|A,A\rangle$, whereas the nonradiative interdot exciton $|B,A\rangle$ is due to exciton tunneling from higher energy states of the QD B to lower energy state of QD A in the coupled conditions.[6,9,10] Because of this dominating intradot exciton $|A,A\rangle$ and interdot exciton $|B,A\rangle$ resulting from coupling of two QDs A and B, one can

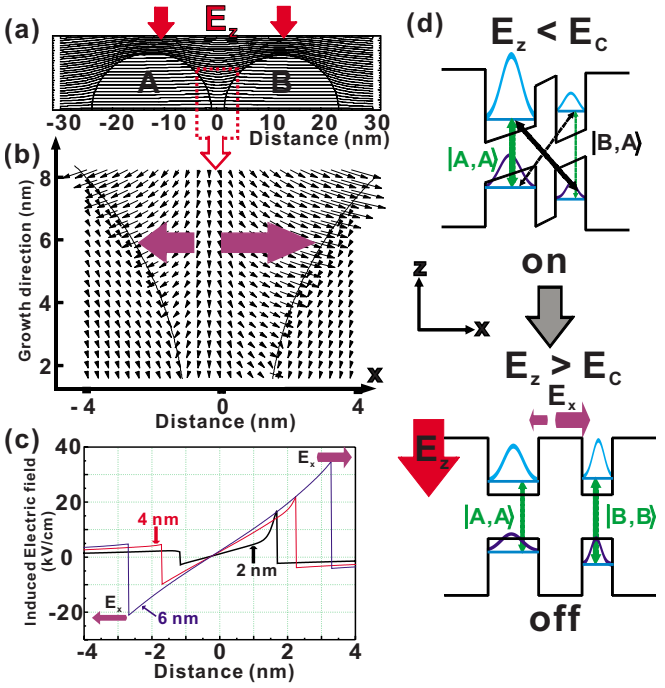

FIG. 4. (Color online) (a) Calculated contour plot of the potential of the induced lateral electric field between QDs located closely nearby. The vertical electric field along the z direction is also shown. (b) Vector plot of the laterally induced electric-field components in the center area of two QDs. (c) Cross-sectional profile of the electric field along the x axis of (b) with respect to the distance between QDs A and B at 2, 4, and 6 nm growth direction. Here the positive (negative) electric field denotes the field direction in the positive (negative) x direction of (a) and (b). (d) Sketch of the lateral QD potential structure for the coupled condition as well as the collapse condition with respect to the critical external electric field (E_C).

observe the dominant PL peaks of A occur without external electric field or under an external electric field smaller than −46 kV/cm in Fig. 3(g), (1)–(4). On the other hand, when the electric field is −92 kV/cm, the maximum lateral electric field of the QDs A and B in Fig. 4(c) is, respectively, induced at about −2 kV/cm (−9 and −21 kV/cm) and 16 kV/cm (22 and 34 kV/cm) with opposite inner direction of each QDs at 2 nm (4 and 6 nm) growth direction from GaAs buffer layer as Fig. 4(b). This induced electric field collapses the coupling between A and B while it increases the potential barrier between coupled QDs as shown in the bottom of Fig. 4(d). In other words, because of this removal of the coupling between two QDs, the nonradiative interdot exciton $|B,A\rangle$ is rapidly decreased and the radiative intradot exciton $|B,B\rangle$ becomes dominant. Consequently we can understand the lower intensity and the appearance of PL-intensity image of A and B in Fig. 3(g), (5) and (6) as due to the field-induced collapse of coupling. Note that the induced lateral electric field inside each QDs, which is about several tens of kilovolt per centimeter in Fig. 4, is strong enough to break the coupling between QDs A and B in comparison with the electric field used for formation of coupling between QDs.[6–9] And since this induced electric field break the coupling condition

and simultaneously compress the lateral PW of each QDs in direction of induced electric field, we could also observe the continuous redshifted of PL peaks of A and B under −15 to ~−184 kV/cm as shown Figs. 2(a) and 2(c). Note also that with applying −138 and −184 kV/cm, we could observe the rapid disappearing of the PL peak of A compared to B, which is due to the reduction in exciton confine in Fig. 3(g), (7)–(10). This indicates that the exciton in A is more weakly confined than that in B because of the larger lateral size of the QD A.[27] Therefore, we could confirm that the variation in the PL spectra and the PL-intensity images in Fig. 3 represents the electric-field-induced formation (*on* condition) or the removal (*off* condition) of the coupling between QDs A and B, where the switching occurs at near the critical electric field.

IV. CONCLUSION

We have observed the spatial PL-intensity images which directly represent the electric-field-induced optical switching due to formation (on condition) and collapse (off condition) of the coupling between laterally neighboring QDs in a self-assembled, high-density QD sample. This work may open the possibility to investigate the coupling interactions between closely neighboring QDs in a high-density QD sample for quantum optics or quantum information applications.

ACKNOWLEDGMENTS

This work was supported by the Acceleration Research Program of the Korea Science and Engineering Foundation. W.J. is grateful for the support of LG Yonam Foundation.

*Present address: Department of Physics, Columbia University, New York, New York 10027, USA.
†Present address: Park Systems Corp., Suwon 443-270, Korea.
‡Corresponding author; whjhe@snu.ac.kr

[1] A. Zrenner, E. Beham, S. Stufler, F. Findeis, M. Bichler, and G. Abstreiter, Nature (London) **418**, 612 (2002).
[2] E. Biolatti, R. C. Iotti, P. Zanardi, and F. Rossi, Phys. Rev. Lett. **85**, 5647 (2000).
[3] B. W. Lovett, J. H. Reina, A. Nazir, and G. A. D. Briggs, Phys. Rev. B **68**, 205319 (2003).
[4] A. Imamoglu, D. D. Awschalom, G. Burkard, D. P. DiVincenzo, D. Loss, M. Sherwin, and A. Small, Phys. Rev. Lett. **83**, 4204 (1999).
[5] R. Heitz, I. Mukhametzhanov, P. Chen, and A. Madhukar, Phys. Rev. B **58**, R10151 (1998).
[6] G. Ortner, M. Bayer, Y. Lyanda-Geller, T. L. Reinecke, A. Kress, J. P. Reithmaier, and A. Forchel, Phys. Rev. Lett. **94**, 157401 (2005).
[7] H. J. Krenner, M. Sabathil, E. C. Clark, A. Kress, D. Schuh, M. Bichler, G. Abstreiter, and J. J. Finley, Phys. Rev. Lett. **94**, 057402 (2005).
[8] G. Schedelbeck, W. Wegscheider, M. Bichler, and G. Abstreiter, Science **278**, 1792 (1997).
[9] G. J. Beirne, C. Hermannstädter, L. Wang, A. Rastelli, O. G. Schmidt, and P. Michler, Phys. Rev. Lett. **96**, 137401 (2006).
[10] T. Kawazoe, K. Kobayashi, S. Sangu, and M. Ohtsu, Appl. Phys. Lett. **82**, 2957 (2003).
[11] M. Reischle, G. J. Beirne, R. Roßbach, M. Jetter, H. Schweizer, and P. Michler, Phys. Rev. B **76**, 085338 (2007).
[12] K. Nishibayashi, T. Kawazoe, M. Ohtsu, K. Akahane, and N. Yamamoto, Appl. Phys. Lett. **93**, 042101 (2008).
[13] A. Dousse, L. Lanco, J. Suffczyński, E. Semenova, A. Miard, A. Lemaître, I. Sagnes, C. Roblin, J. Bloch, and P. Senellart, Phys. Rev. Lett. **101**, 267404 (2008).
[14] M. Bayer, P. Hawrylak, K. Hinzer, S. Fafard, M. Korkusinski, Z. R. Wasilewski, O. Stern, and A. Forchel, Science **291**, 451 (2001).
[15] H. Saito, K. Nishi, and S. Sugou, Appl. Phys. Lett. **73**, 2742 (1998).
[16] Y.-J. Yu, H. Noh, M.-H. Hong, H.-R. Noh, Y. Arakawa, and W. Jhe, Opt. Commun. **267**, 264 (2006).
[17] Y.-J. Yu, W. Jhe, and Y. Arakawa, Appl. Phys. Lett. **83**, 3024 (2003).
[18] Y.-J. Yu, H. Noh, G. S. Jeon, H.-R. Noh, Y. Arakawa, and W. Jhe, Appl. Phys. Lett. **91**, 041117 (2007).
[19] K. Matsuda, T. Saiki, S. Nomura, M. Mihara, Y. Aoyagi, S. Nair, and T. Takagahara, Phys. Rev. Lett. **91**, 177401 (2003).
[20] Y. Sugimoto, T. Saiki, and S. Nomura, Appl. Phys. Lett. **93**, 083116 (2008).
[21] E. S. Moskalenko, M. Larsson, W. V. Schoenfeld, P. M. Petroff, and P. O. Holtz, Phys. Rev. B **73**, 155336 (2006).
[22] S. Laurent, B. Eble, O. Krebs, A. Lemaître, B. Urbaszek, X. Marie, T. Amand, and P. Voisin, Phys. Rev. Lett. **94**, 147401 (2005).
[23] I. Shtrichman, C. Metzner, B. D. Gerardot, W. V. Schoenfeld, and P. M. Petroff, Phys. Rev. B **65**, 081303 (2002).
[24] M. Baier, F. Findeis, A. Zrenner, M. Bichler, and G. Abstreiter, Phys. Rev. B **64**, 195326 (2001).
[25] A. Goyette and A. Navon, Phys. Rev. B **13**, 4320 (1976).
[26] P. C. Chaumet and J. P. Dufour, J. Electrost. **43**, 145 (1998).
[27] H. Gotoh, H. Kamada, H. Ando, and J. Temmyo, Appl. Phys. Lett. **76**, 867 (2000).